Metallic Liquids and Glasses: Atomic Order and Global Packing

X. J. Liu,[1,2] Y. Xu,[1] X. Hui,[1] Z. P. Lu,[1,*] F. Li,[3] G. L. Chen,[1,†] J. Lu,[2] and C. T. Liu[2,‡]

[1]*State Key Laboratory for Advanced Metals and Materials, University of Science and Technology Beijing, Beijing 100083, China*
[2]*Department of Mechanical Engineering, The Hong Kong Polytechnic University, Hung Hom, Kowloon, Hong Kong, China*
[3]*Engineering Research Center of Materials Behavior and Design, Nanjing University of Science and Technology, Nanjing 210094, China*

(Received 3 May 2010; revised manuscript received 16 July 2010; published 5 October 2010)

In this Letter, we have revealed the common structural behavior of metallic glasses through scrutinizing the evolution of pair distribution functions from metallic liquids to glasses and statistically analyzing pair distribution functions of 64 metallic glasses. It is found that the complex atomic configuration in metallic glasses can be interpreted *globally* as a combination of the spherical-periodic order and local translational symmetry. The implications of our study suggest that the glass transition could be visualized mainly as a process involving in local translational symmetry increased from the liquid to glassy states.

DOI: 10.1103/PhysRevLett.105.155501 PACS numbers: 61.43.Dq, 61.43.Bn

The atomic structure of metallic glasses (MGs) is a fundamental and intriguing issue in condensed-matter physics, due to its importance in understanding the glass-forming mechanism and unique properties [1–4]. Many structural models have been proposed over the years, such as ''dense random packing'' of hard spheres [5] and the ''stereochemically designed'' model [6]. Although these early models significantly improved our understanding of atomic structures in MGs, especially for short-range order (SRO), they still have their own insufficiencies [7]. Recent studies confirm that the characteristics of medium-range order (MRO) clusters dictate the stability and mechanical properties of monolithic MGs [8–11], which have shed new light on our understanding of structural features at this length scale [7,12–14]. By taking the earlier models further with advances in relevant experimental techniques and computational capacity, the idealized cluster packing schemes, such as efficient cluster packing on a face-centered cubic (fcc) lattice [12] and quasiequivalent clusters on an icosahedral packing [7], have been proposed and furthered our comprehension of the MRO. However, the latest finding indicated that the MRO in MGs can be described by packing of quasiequivalent clusters on a fractal network with a dimension (D_f) of 2.31 [14], implying that it is impossible to fill the real space in these amor phous solids by building blocks in a form of crystal ($D_f = 3.0$) or icosahedral-quasicrystal ($D_f = 2.72$) symmetry. The nature of atomic packing at the MRO scale or larger in MGs still remains mysterious [15].

Glassy alloys are commonly considered as the state of ''frozen liquids''; nevertheless, their structure difference is obvious: A split in the second peak of the atomic-pair distribution function (PDF) curve, $g(r)$, for MGs, occurs with respect to that for liquids. Actually, the splitting of the second maximum of the $g(r)$ curve into two subpeaks is recognized as a characteristic indication of amorphous solids [16], and its origin has been investigated extensively [17–19]. For example, Bennett proposed that the first subpeak at $R_2/R_1 = \sqrt{3}$ results from a continuum of configuration of two coplanar equilateral triangles sharing a common side, and the second one at $R_3/R_1 = \sqrt{4}$ originates from the linear array of three spheres [18]. Recently, Voloshin and Naberukhin attributed the splitting-forming atomic configurations to chains of tetrahedra and/or quartoctahedra [19]. Obviously, these analyses focused on extremely localized atomic packing, and a global description is still missing. On the other hand, considering the electronic influence on structure, Häussler indicated that both the SRO and MRO in ideal disordered systems, such as liquid and amorphous solids, could be described globally by the so-called spherical-periodic order (SPO) [20]; nevertheless, such spherical periodicity does not weigh the local crystallinelike ordering which is commonly found in both theoretical investigations [21,22] and experimental observations [23–26]. Inspired by the splitting of the second peak in $g(r)$ of MGs and the SPO of atomic packing in disordered solids, we initially scrutinized the $g(r)$ evolution from metallic liquids to glasses in monatomic systems by molecular dynamics (MD) simulations and then collected and statistically analyzed numerous PDF data of various multicomponent MGs in the literature. From these studies, we revealed a global feature of the PDFs for all MGs and further demonstrated that this global feature can be well characterized by the combination of SPO and local translational symmetry (LTS). From the atomic structure perspective, our finding suggests that the nature of a glass transition could be a process associated with the increase of LTS imposed on the SPO.

Although the difference in $g(r)$ between metallic liquids and glasses has been recognized [16], the structural evolution following the liquid-glass transition is far from being fully understood. To address this issue, we investigated the glass-forming process of several pure metals, including Ni, Al, and Cu, through analyzing their PDF curves obtained

from MD simulations [27]. As an example, Fig. 1 shows the MD modeled $g(r)$ curves for the liquid and glassy states of pure Ni. Only two pronounced oscillation peaks in the PDF can be seen for the liquid state while at least five ones for the glassy state. The second peak in the liquid state is split into two subpeaks in the glassy state, and the peak intensities in the glassy state are stronger than those in the liquid state. In all three metal systems, similar results were observed, which implies that the glassy state has a higher degree of order with respect to the liquid state. The absolute values of R_i vary with composition; for example, R_1 shifts from 2.47 Å in the glassy Ni to 2.85 Å in the glassy Al. In view of the physical definition of a PDF, R_i always represents the average distance from the ith nearest-neighbor shell to the centered atom. For instance, the R_1 corresponds to the average distance of the first nearest-neighbor shell. Therefore, by normalizing all the peak positions to R_1 in real PDF patterns, we can minimize the influences of the chemical composition and atomic size on the peak positions and thus extract the general features of different alloy systems. In light of this consideration, we calculated the ratios of R_i/R_1 ($i = 1, 2$ for liquids and $i = 1$–5 for solid glasses) for these systems. Here, R_i was obtained by fitting the corresponding peak using a Gaussian function. For instance, the R_2 and R_3 were determined by fitting the splitting second peak in the $g(r)$ with two overlapping Gaussian functions [14]. As expected, a scaling behavior of R_i/R_1 is found to be the general feature of PDFs for both the liquid and glassy states. Namely, the ratios of R_1/R_1 and R_2/R_1 are of 1.0 and 1.86, respectively, for all the liquids, while the values of R_i/R_1 ($i = 1$–5) for all the monolithic MGs are surprisingly found to be close to the constants of 1.0 ($\sqrt{1}$), 1.73 ($\sqrt{3}$), 2.0 ($\sqrt{4}$), 2.64 ($\sqrt{7}$), and 3.46 ($\sqrt{12}$), respectively.

Then, it is important to know whether this scaling behavior of R_i/R_1 still holds well in PDFs for complex alloy systems, such as the realistic bulk metallic glasses prepared experimentally in the laboratory. To answer this question, we determined PDFs for $Zr_{38.2}Cu_{61.8}$, $Zr_{44}Cu_{56}$, $Zr_{66.7}Ni_{33.3}$, and $Zr_{40}Cu_{55}Al_5$ (at. %) MGs by synchrotron x-ray scattering experiments [27] and statistically analyzed 57 sets of data from the literature (see Table S1 in Ref. [27]). Figure 2 is the statistical results of the R_i/R_1 ratios ($i = 1$–5) obtained from the PDF patterns of all 64 amorphous alloys shown in Table S1. Note that Fig. 2 illustrates the data for a large variety of MGs ranging from unary and binary alloys with marginal glass-forming ability to multicomponent bulk metallic glasses with good glass-forming ability, including pure metals, Zr-, Cu-, Ni-, Fe-, Al-, and Pd-based metal-metal, and metal-metalloid MGs. From Fig. 2, it is amazing to observe that the statistical results are in excellent agreement with the aforementioned results for monatomic systems; that is, R_i/R_1 ratios are not continuous but correspond to several characteristic values, namely, $\sqrt{1}$, $\sqrt{3}$, $\sqrt{4}$, $\sqrt{7}$, and $\sqrt{12}$, although the absolute value of R_1 increases from 2.41 to 3.11 Å for various alloy systems. Meanwhile, we verified that the experimental PDF profile is slightly changed with different radiation resources, but, in principle, the peak position R_i is not strongly affected by the radiation resource [27]. This is because R_i represents atomic-pair distance, which is not affected by the radiation resource. As a result, effects of the radiation sources on the ratios of R_i/R_1 are ignorable. Obviously, this scaling behavior of R_i/R_1 is a universal feature in MGs, which is independent of alloy compositions and atomic sizes.

In disordered metallic systems, such as liquids or ideal amorphous metals, due to the electronic influences on the interatomic potential, there exist so-called spherical Friedel oscillations in the effective pair potential [20], which cause the SPO of atomic arrangement at the short- and medium-range distances. According to the spherical-periodic arrangement, the nearest-neighbor positions locate at the distances R_n^{SPO} [20]:

$$R_n^{\mathrm{SPO}} = (1/4 + n)\lambda_F (n = 1, 2, 3 \ldots), \quad (1)$$

where $\lambda_F = 2\pi/2k_F$ is the Friedel wavelength and $2k_F$ is the Fermi-sphere diameter. Based on Eq. (1), the SPO

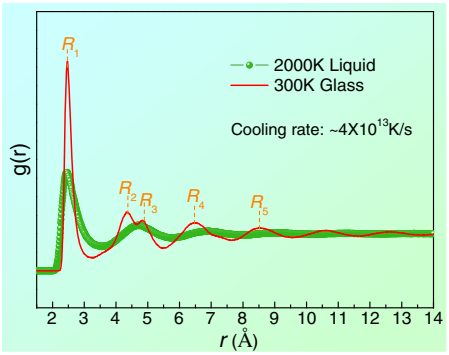

FIG. 1 (color online). MD modeled $g(r)$ curves of metal Ni for the liquid at 2000 K and amorphous state 300 K. The short dashed lines schematically indicate the peak positions.

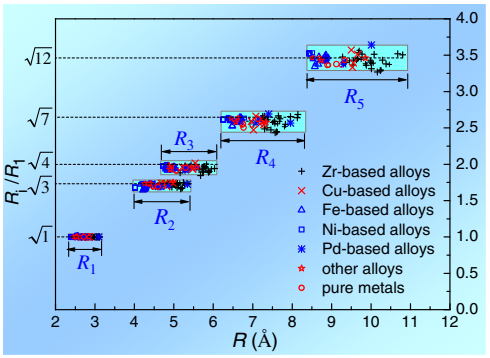

FIG. 2 (color online). Ratio of peak positions normalized to the first peak R_i/R_1 for 64 MGs ranging from unary to quinary systems. The blue rectangles are drawn to guide the eyes.

theory predicts the $R_n^{\mathrm{SPO}}/R_1^{\mathrm{SPO}}$ ($n = 1, 2, 3, 4$) values are of 1.0, 1.8, 2.6, and 3.4 as n varies from 1 to 4, respectively. By comparing the statistical values in Figs. 1 and 2 with the SPO prediction, it is found that the first two neighbor shells in the liquid state could be predicted by the SPO theory very well. For MGs, the predicted values are basically consistent with the aforementioned values of 1.0 ($\sqrt{1}$), 1.73 ($\sqrt{3}$), 2.64 ($\sqrt{7}$), and 3.46 ($\sqrt{12}$) as shown in Fig. 2, except for the ratio of R_3/R_1 ($\sqrt{4}$). This comparison indicates that the SRO structure in metallic liquids can be well described by SPO arrangement, but an additional order or symmetry seemingly emerges in addition to the basic SPO during the glass transition.

In fact, the glass formation could be considered as a process of hidden crystalline ordering under frustration [21,22], and the long-lived medium-range crystalline order (MRCO) has been observed directly in a model liquid near the glass transition temperature [25]. In realistic multicomponent glass-forming liquids, the MRCOs are thus expected to be more pronounced due to the chemical interactions among unlike constituents, and these MRCOs will be retained in the glassy state upon cooling. As a result, the MRCO domains with a size of 1–2 nm are frequently observed in bulk metallic glasses [28,29]. Therefore, the assumption that there exists a localized crystallinelike order in realistic MGs is reasonable. Because of the requirement of atomic dense packing, the MRCO in MGs is expected to be fcc or hexagonal closest packing (hcp) type as much as possible, which is consistent with previous experimental observations [28,29]. According to the characteristics of a dense-packed lattice (the fcc lattice as an example in Fig. 3), it is ready to deduce two kinds of packing: One is the atomic packing with relative position ratios of $\sqrt{1}$, $\sqrt{3}$, $\sqrt{5}, \ldots$, which is comprised of atoms arranged along the dense-packed directions in the fcc lattice (yellow atoms in Fig. 3), and the other is the atomic packing with the relative position ratios of $\sqrt{2}$, $\sqrt{4}$, $\sqrt{6}, \ldots$, which consists of atoms located at lattice point positions (green atoms in Fig. 3). It is clear that the R_3/R_1 ratio of $\sqrt{4}$ that cannot be predicted by the SPO theory may arise from the crystallinelike (such as fcc-like) order. Furthermore, it should be noted that this crystallinelike order is a LTS due to the following facts. (i) Only the lattice point that constructs the crystal structure along the dense-packed direction is occupied by atoms; that is, only $\sqrt{4}$ (along $\langle 110 \rangle$) occurs but no others [such as $\sqrt{2}$ (along $\langle 100 \rangle$)]. In other words, the LTS represents only one-dimensional (1D) translational order along a dense-packed direction rather than 3D translational periodic order in a lattice. Therefore, it is not necessary for the MRCOs in MGs to be fcc or hcp type, provided that the 1D LTS could be developed. (ii) The translational ordering is localized, and its scale does not exceed the fourth neighbor (distance at $\sqrt{5}R_1$) in an fcc lattice due to the frustration effects of locally favorable SRO (such as the icosahedral order) on the crystalline long-range ordering (see Ref. [21]).

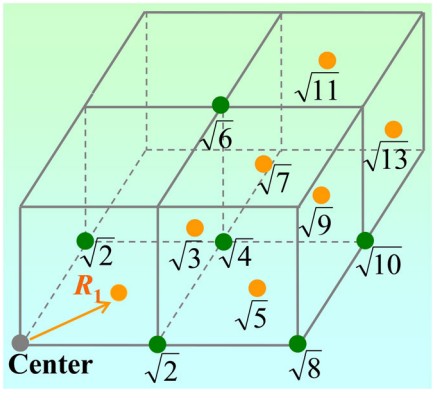

FIG. 3 (color online). The sketch of a face-centered cubic lattice and the illustration of a given centered atom (gray) and the atoms located at the face-centered positions (yellow) and at the sites of lattice point positions (green). The numbers labeled on the atoms represent the normalized values of their distances away from the centered atom to R_1.

Based on the illustration above, it is reasonable to propose that the atomic packing in MGs is a result of the superimposition of LTS on the basic SPO. Figure 4 provides solid evidence to support this claim, which contains 4 neighboring shells consisting of 150 atoms around a center atom [the red one in Fig. 4(a)], and was randomly picked out from the MD modeled Ni glass system with 4000 atoms in total. Figure 4(b) shows the calculated PDF curve of Fig. 4(a), which exhibits an obvious R_3 peak (as indicated by the green arrow) originating from the LTS atomic packing. Figure 4(c) definitely identifies the combination of SPO (marked with red dashed lines) and LTS (marked with blue rectangles) structural features in the Ni glass. For multicomponent MGs, their atomic structures are very complicated and contain free volume, various complex SROs and MROs due to the chemical and topological effects [9,14–16]. By scaling R_i to R_1, however, one can still extract the global feature from the complex atomic structure as evidenced by the statistical results (Fig. 2). This demonstrates that the global scheme of atomic packing characterized by the combination of SPO and LTS is still applicable in the multicomponent systems, although their PDF profiles could be more complex than those in the monatomic ones.

The electron distribution in disordered metallic systems is the origin of the SPO [20], which is considered as the basic, characteristic structural feature of condensed matter at early stages [30]. In order to minimize the total system energy, there is a self-organized optimization process of the spherical resonances between the valance electrons and static structure during the formation of condensed phases. As the first stage of condensed matter, the liquid state can be well described by the basic SPO as confirmed in our case. The optimization process proceeds further during

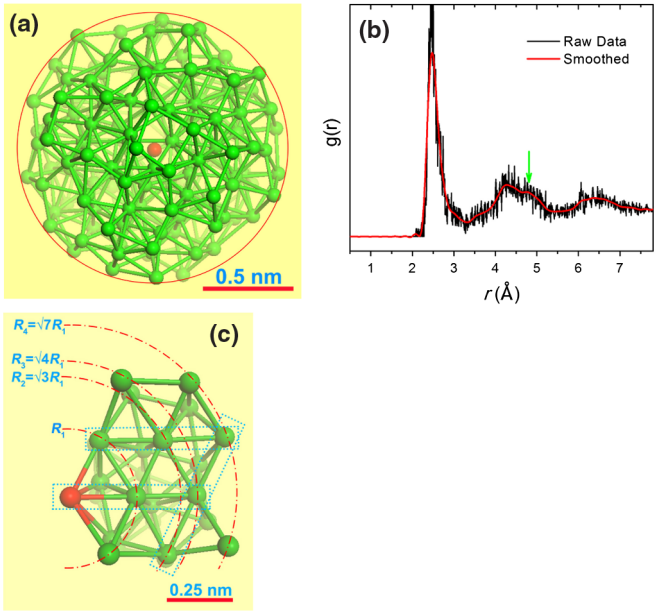

FIG. 4 (color online). (a) Atomic configuration of a local cluster including 150 atoms picked out from the MD modeled Ni glass. (b) Calculated PDF curve of (a); the green arrow points out the R_3 peak. (c) Atomic configuration of one quadrant of (a); the red dashed lines and blue rectangles mark the SPO and LTS features, respectively.

undercooling of the liquid, leading to a relatively higher degree of order in the new phase. If the optimization process is completed, the stable crystalline structures are developed. Since the glassy state is an intermediate step between the liquid and the crystalline, the degree of order in MGs is higher than that in liquids but still lower than that in crystals. On the other hand, the chemical interactions between constituents will contribute to the formation of LTS. In fact, from the phase competition point of view, glass formation could be considered as a process of hidden crystalline ordering under frustration [21,22], which is why the second peak of the liquid state is split into two subpeaks in the glassy state (as shown in Fig. 1). Based on our finding, therefore, the glass transition could be virtually regarded as a process to increase the LTS on the basis of the spherical periodicity, from an atomic structure perspective.

In summary, we have revealed a *global* structural feature for various MGs through statistically analyzing a variety of PDF data and MD simulations. The results demonstrate that the atomic packing in MGs can be described *globally* as the LTS superimposed on the SPO. In the sense of atomic structure, our results indicate that a glass transition is a process of increasing the LTS on the basis of SPO. This finding could shed new light on the nature of atomic structures and has very important implications in understanding the fundamental mechanism governing the formation of various MGs.

This work was supported by the NSFC (No. 50725104 and No. 50901006), the RFDP (No. 20090006120025), and the 111 Project (No. B07003). X. J. L. is also supported by the SKLAMM at USTB and internal funding from PolyU. C. T. L. and J. L. are also supported by the internal funding from PolyU. Help from Professor Y. D. Wang in synchrotron experiments and fruitful discussions with Professor M. W. Chen and Dr. S. Guo are highly appreciated.

*To whom correspondence should be addressed.
luzp@ustb.edu.cn
†glchen@skl.ustb.edu.cn
‡liuct@ornl.gov

[1] A. Inoue, Acta Mater. **48**, 279 (2000).
[2] W. H. Wang, C. Dong, and C. H. Shek, Mater. Sci. Eng., R **44**, 45 (2004).
[3] A. L. Greer and E. Ma, MRS Bull. **32**, 611 (2007).
[4] T. Fujita *et al.*, Phys. Rev. Lett. **103**, 075502 (2009).
[5] J. D. Bernal, Nature (London) **185**, 68 (1960).
[6] P. H. Gaskell, Nature (London) **276**, 484 (1978).
[7] H. W. Sheng *et al.*, Nature (London) **439**, 419 (2006).
[8] A. R. Yavari, Nature (London) **439**, 405 (2006).
[9] C. E. Lekka *et al.*, Appl. Phys. Lett. **91**, 214103 (2007).
[10] Y. Q. Cheng, H. W. Sheng, and E. Ma, Phys. Rev. B **78**, 014207 (2008).
[11] X. D. Wang *et al.*, Appl. Phys. Lett. **94**, 011911 (2009).
[12] D. B. Miracle, Nature Mater. **3**, 697 (2004).
[13] X. J. Liu *et al.*, Appl. Phys. Lett. **93**, 011911 (2008).
[14] D. Ma, A. D. Stoica, and X. L. Wang, Nature Mater. **8**, 30 (2009).
[15] D. B. Miracle *et al.*, MRS Bull. **32**, 629 (2007).
[16] R. Zallen, *The Physics of Amorphous Solids* (Wiley, New York, 1983).
[17] J. L. Finney, Proc. R. Soc. A **319**, 479 (1970).
[18] C. H. Bennett, J. Appl. Phys. **43**, 2727 (1972).
[19] V. P. Voloshin and Y. I. Naberukhin, J. Struct. Chem. **38**, 62 (1997).
[20] P. Häussler, Phys. Rep. **222**, 65 (1992).
[21] H. Shintani and H. Tanaka, Nature Phys. **2**, 200 (2006).
[22] T. Kawasaki, T. Araki, and H. Tanaka, Phys. Rev. Lett. **99**, 215701 (2007).
[23] N. Mattern *et al.*, Acta Mater. **50**, 305 (2002).
[24] X. J. Liu *et al.*, Phys. Lett. A **372**, 3313 (2008).
[25] K. Watanabe and H. Tanaka, Phys. Rev. Lett. **100**, 158002 (2008).
[26] P. Wochner *et al.*, Proc. Natl. Acad. Sci. U.S.A. **106**, 11 511 (2009).
[27] See supplementary material at http://link.aps.org/supplemental/10.1103/PhysRevLett.105.155501 for the experimental and simulation details.
[28] G. L. Chen *et al.*, Appl. Phys. Lett. **88**, 203115 (2006).
[29] A. Hirata *et al.*, Ultramicroscopy **107**, 116 (2007).
[30] P. Häussler, in *Proceedings of the 11th International Conference on Phonon Scattering in Condensed Matter*, edited by A. Kaplyanskii, A. Akimov, and V. Bursian (Wiley-VCH, Weinheim, 2004), pp. 2879.